SUPPORTING INFORMATION

Catalytic mechanism and allosteric regulation of UDP-glucose pyrophosphorylase from *Leishmania major*

Jana Führing[1], Johannes T. Cramer[1], Françoise H. Routier[1], Anne-Christin Lamerz[1,†], Petra Baruch[2], Rita Gerardy-Schahn[1] and Roman Fedorov[2,3]*

[1] Institute for Cellular Chemistry, OE4330, Hannover Medical School, Carl-Neuberg-Strasse 1, 30625 Hannover, Germany

[2] Research Division for Structural Analysis, OE8830, Hannover Medical School, Carl-Neuberg-Strasse 1, 30625 Hannover, Germany

[3] Institute for Biophysical Chemistry, OE4350, Hannover Medical School, Carl-Neuberg-Strasse 1, 30625 Hannover, Germany

Corresponding Author

[*] Roman Fedorov, Research Division for Structural Analysis, OE8830, Hannover Medical School, Carl-Neuberg-Strasse 1, 30625 Hannover, Germany

Phone: +49-5115323705; Fax: +49-5115325966; E-mail: Fedorov.Roman@mh-hannover.de

TABLE OF CONTENTS

TABLES

FIGURES

TABLES

Supplementary Table S1. Crystallographic data and refinement statistics

Protein / Complex	$LmUGP_{H191L}$	$LmUGP_{wt}$· dUpCpp	$LmUGP_{L281D}$· UDP-Glc	$LmUGP_{wt}$·UDP-Glc·Mg·SO_4
PDB-code	4J18	4M28	4M2B	4M2A
Crystal parameters				
Group	*$P4_3$*	*$C222_1$*	*$C222_1$*	*$C222_1$*
Cell parameters: a, b, c, [Å] α, β, γ [º]	101.3, 101.3, 71.8, 90, 90, 90	72.3, 108.5, 152.6, 90, 90, 90	78.8, 86.9, 138.2, 90, 90, 90	79.8 89.1 136.5, 90, 90, 90
Data collection				
Beamline	ID29, ESRF	ID23-2, ESRF	X11, DESY	X13, DESY
Wavelength (Å)	0.91985	0.87260	0.816	0.806
Resolution limit (high-resolution shell) (Å) *	2.35 (2.4-2.35)	3.0 (3.1-3.0)	2.2 (2.25-2.2)	1.66 (1.75-1.66)
No. of observations / unique reflections	111527 / 30206	126117 / 11151	213348 / 24483	1108570 / 57313
Completeness (total / high) %	99.2 / 98.2	90.0 / 89.0	98.0 / 97.5	99.7 / 97.9
$\langle I/\sigma(I)\rangle$ (total / high)	9.8 / 2.4	11.6 / 3.4	14.4 / 4.0	28.8/ 8.8
R_{sym} (total / high) %	10.4 / 48.6	8.0 / 40.7	7.6 / 27.1	2.3 / 12.1
Refinement statistics				
Resolution range (Å)	19.5 – 2.35	47.3 – 3.0	69.1 – 2.2	68.3 – 1.66
Included amino acids	4 - 488	6 - 488	6 – 488	6-488
No. of protein atoms	4059	3730	3730	3730
No. of waters	418	77	393	665
R_{work} / R_{free} %	17.8 / 23.2	21.3 / 27.9	17.5 / 24.2	19.0 / 24.7
r.m.s.d. bonds (Å) / angles (deg)	0.018 / 2.1	0.009 / 1.2	0.007 / 1.4	0.005 / 1.2

*) High-resolution cutoffs were applied to resolution shells which had Rsym ≥ 50% or had sustained high radiation damage.

Supplementary Table S2. Absolute QM/MM DFT (B3LYP5) energies computed for the LmUGP reagents, transition state and products geometries resulting from the IRC calculations

Geometry along the reaction pathway of LmUGP	Electronic energy (a.u.)	Gibbs energy using harmonic normal mode approximation (kcal/mol)
Reagents	-3117.780642	-1953475.781
Transition state	-3117.746956	-1953455.003
Products	-3117.777507	-1953477.246

FIGURES

Supplementary Figure S1 A

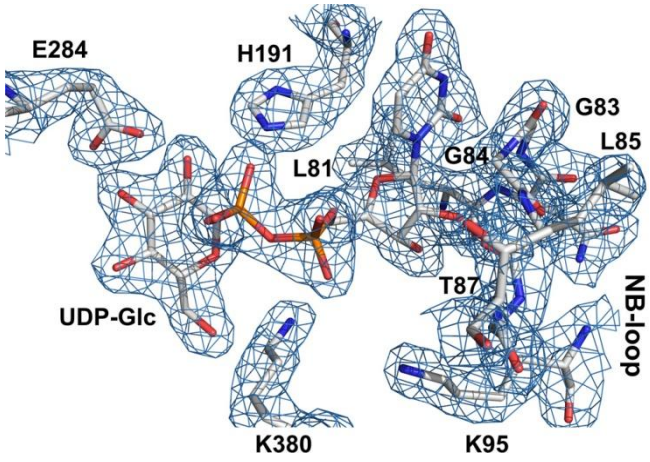

Supplementary Figure S1 B

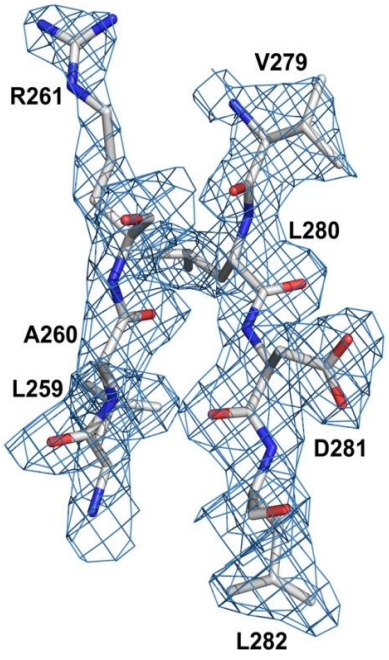

Supplementary Figure S1 C

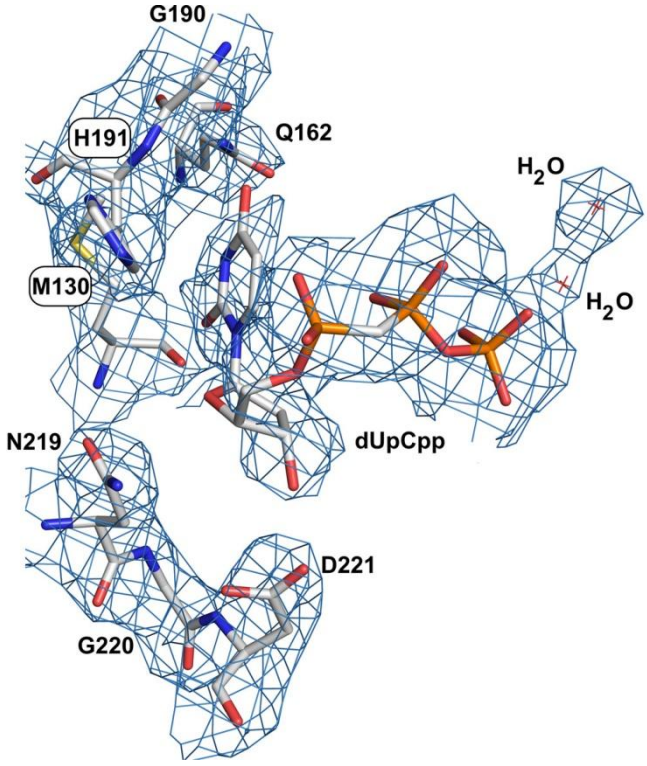

Supplementary Figure S1 D

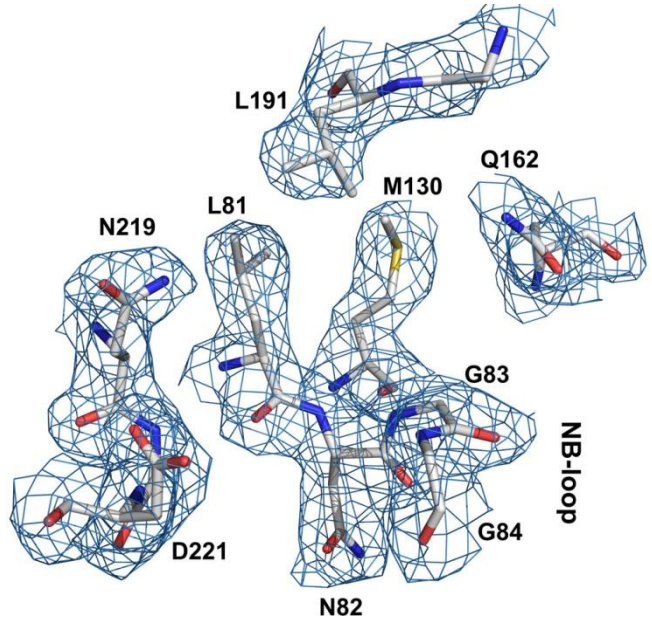

Supplementary Figure S1. Sections of the $2F_{obs} - F_{calc}$ electron density omit maps contoured at 1.0 σ showing the active site of the $LmUGP_{L281D}$ mutant in complex with UDP-Glc (A), the fraction of the handle region near mutation L281D (B), the UTP binding site in the structure of the $LmUGP_{wt}$·dUpCpp complex (C), and the active site residues in the $LmUGP_{H191L}$ mutant structure (D). All maps were calculated using the final models of the complexes with substrates and ions omitted.

Supplementary Figure S2 (A, B)

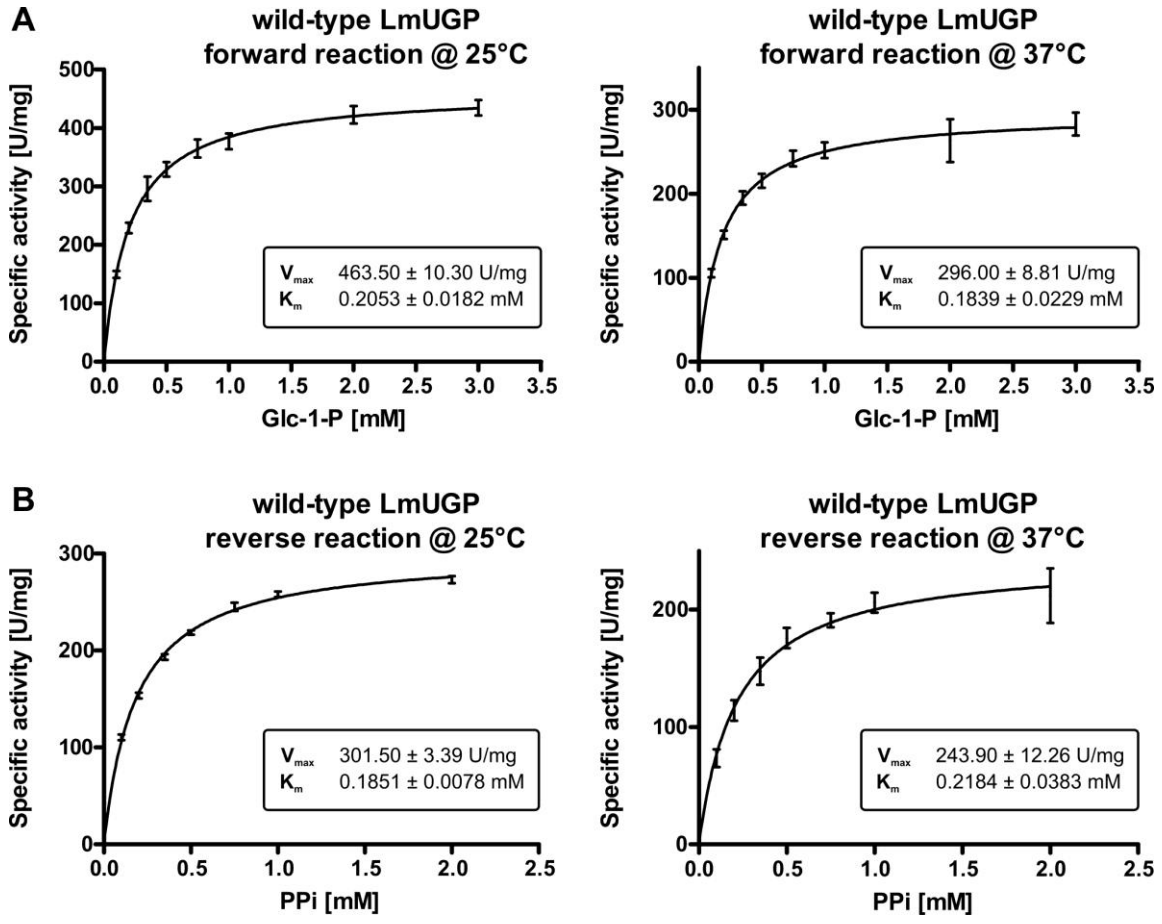

Supplementary Figure S2 (C, D)

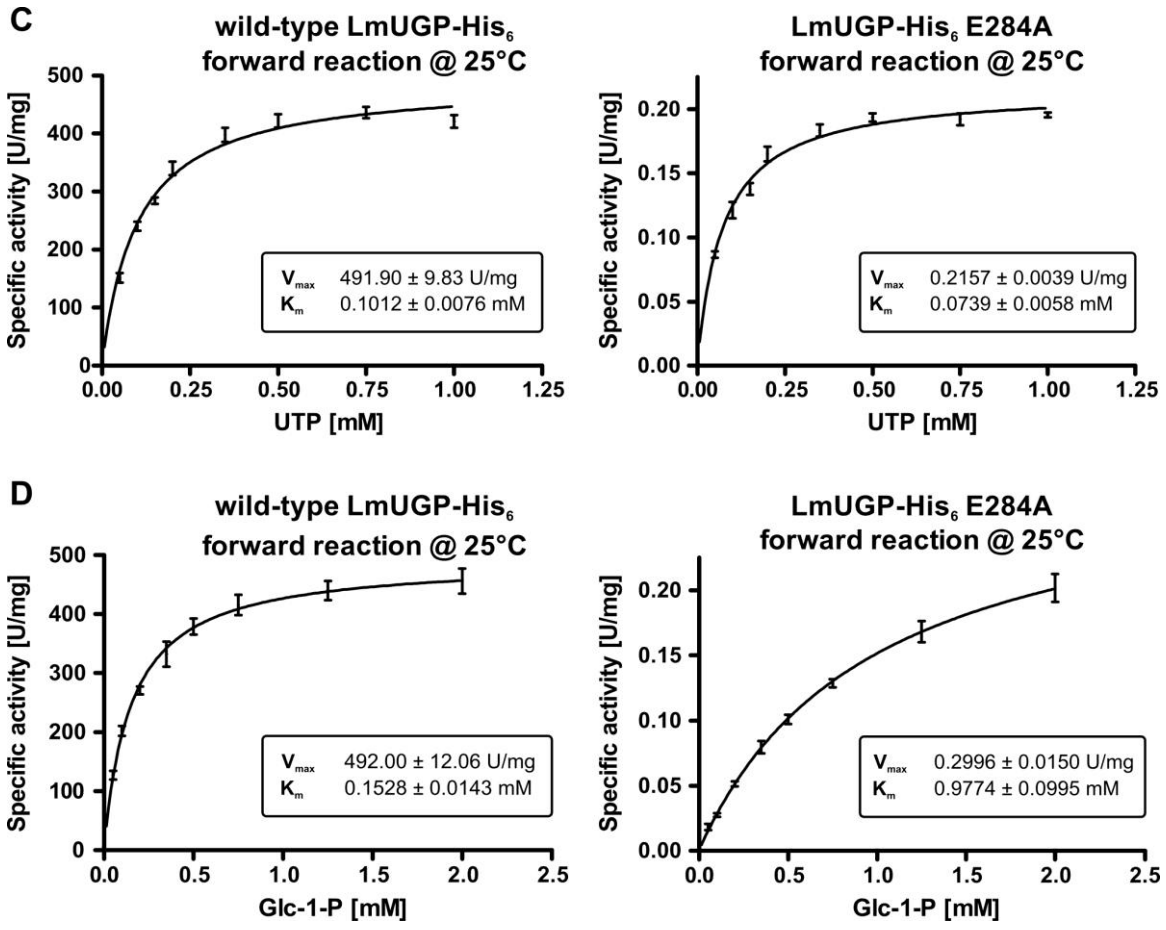

Supplementary Figure S2. Specific activities of wild-type and mutant *Leishmania major* UGP. *In vitro* specific activities, measured in U/mg (y-axis) of untagged and C-terminally His-tagged (LmUGP-His_6) wild-type and mutant LmUGP, were determined in dependence of substrate concentration (x-axis) at different temperatures. V_{max} and K_m values for the varied substrate, determined by nonlinear regression, are given as inlays. Plotting and calculation of kinetic parameters were performed using GraphPad Prism.

Supplementary Figure S3

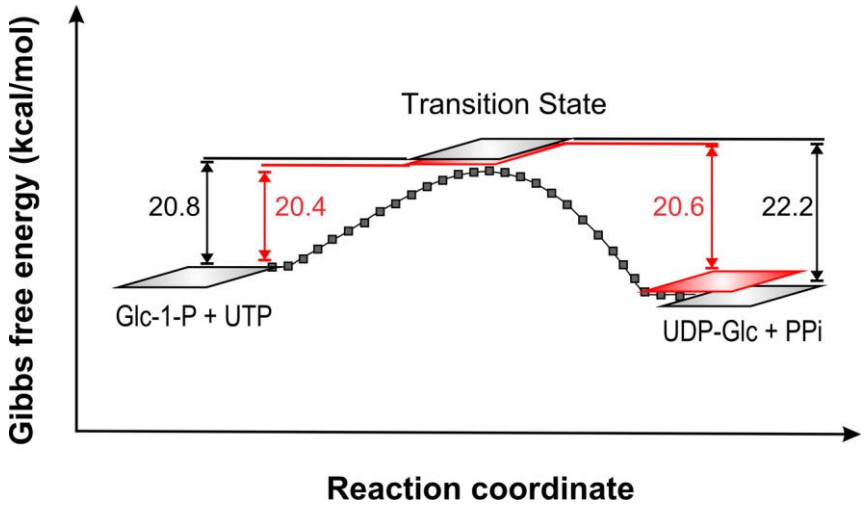

Supplementary Figure S3. Energy profile along the LmUGP reaction pathway. Energy barriers resulting from the quantum chemical calculations (black, **Supplementary Table S2**) are in a good agreement with the barriers derived from experimental kinetics data (red) at a physiological temperature (**Supplementary Fig. S2 A, B** right).

Supplementary Figure S4

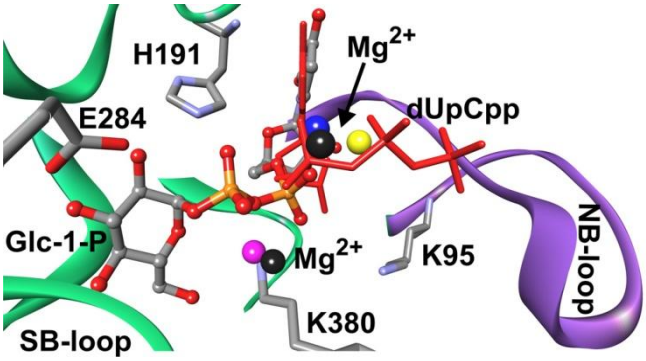

Supplementary Figure S4. Superpositon of LmUGP in the post-reactive state (atom colors: blue, positive; red, negative; grey, neutral; Mg^{2+}, yellow) with LmUGP·dUpCpp complex (only the substrate is shown in red), GMP·GTP complex (pdb-code: 2X60; only Mg^{2+} is shown in blue), GMP·GDP-Man complex (pdb-code: 2X5Z; only Mg^{2+} is shown in magenta) and *C. glutamicum* UGP·UDP-Glc complex (pdb-code: 2PA4; only Mg^{2+} ions are shown in black). The catalytically important Mg^{2+} ions in GMP·GDP-Man and *C. glutamicum* UGP·UDP-Glc complexes occupy the same place as the amino group of K380 side chain in the active conformation of LmUGP.